# A UV Survey of B Supergiants: Time-Averaged Stellar-Wind Properties

Raman K. Prinja

*Dept. of Physics & Astronomy, University College London, Gower Street, London WC1E 6BT, UK*

Derck L. Massa

*Hughes STX, NASA/GSFC, Greenbelt, MD 20771, USA*

**Abstract.** We report on our ongoing quantitative survey of the time-averaged stellar wind properties of Galactic B supergiants, based on high-resolution IUE spectroscopy. Initial results on the wind terminal velocities and the 'bi-stability' region are discussed. The C IV and Si IV resonance-line doublets of B0–B5 supergiants have been modelled using (modified) SEI techniques to provide measures of the product of mass-loss rate and ion fraction ($\dot{M}\, q_i$), and the relative ionization behaviour. The incidence of photospheric velocity gradients is also highlighted.

## 1. Introduction

Luminous B supergiants are excellent candidates for quantitative spectroscopy in the Local Group, providing opportunities to study stellar evolution in different environments, including a wide range of metallicities. They are especially attractive in the ultraviolet since B supergiants are among the most luminous objects at this waveband, thus potentially providing astrophysical diagnostics at large distances.

One of the key observable properties of luminous B stars which is directly accessible from spectroscopy is the nature of their stellar winds. It is ironic, however, that the winds of even *Galactic* B supergiants are not well studied, and these stars have been neglected in most UV mass-loss surveys, which concentrate mainly on O3–B0 spectral types (e.g., Howarth & Prinja 1989, Groenewegen & Lamers 1989). The UV spectroscopic diagnostics available in B-supergiant spectra do, however, present some distinct advantages. Specifically, (*i*) only these stars offer wind properties in such a wide range of *unsaturated* low-ionization (Si III, C II, Al III, Mg II) and high-ionization (N V, Si IV, C IV) lines, (*ii*) their strong UV photospheric Si II and Si III lines are sensitive temperature and surface-gravity diagnostics, and (*iii*) the study of B stars widens the domain over which the theory of radiation-driven stellar winds can be tested; e.g., the effective temperature of these stars varies from ~29 000 K to 10 000 K (for B0–B9), i.e., nearly a factor 3.

Motivated by the necessity for establishing the UV wind properties of B supergiants – and providing an important link to A-type supergiants – we have initiated a quantitative UV survey of the winds of Galactic B0–B9 supergiants, based on high-resolution IUE spectroscopy. Some initial results for B0–B5 stars are reported here, where we have analysed individual spectra for 109 (Ia, Ib, Iab) stars.

Table 1. Mean B-supergiant terminal velocities.

| Sp. type | $\overline{v}_\infty$ (km s$^{-1}$) | Sp. type | $\overline{v}_\infty$ (km s$^{-1}$) |
|---|---|---|---|
| B0 Ia | 1445 | B0 Ib | 1690 |
| B0.5 Ia | 1445 | B0.5 Ib | 1390 |
| B1 Ia | 1210 | B1 Ib | 1010 |
| B1.5 Ia | 780 | B1.5 Ib | 945 |
| B2 Ia | 540 | B2 Ib | 840 |
| B3 Ia | 485 | | |
| B5 Ia | 265 | B5 Ib | 465 |

## 2. Wind Velocities of B Supergiants

Hot-star winds are affected by significant line-broadening mechanisms *other* than macroscopic Doppler broadening due to the bulk velocity field. The non-laminar outflows likely give rise to the formation of forward and/or reverse shocks (e.g., Lucy 1982, 1983; Owocki et al. 1988). In these cases the maximum observed (blue-edge) velocity ($v_{\rm edge}$) can exceed the terminal velocity ($v_\infty$) of the bulk wind. It is generally accepted therefore that reliable measures of $v_\infty$ can be obtained from measures of the shortward edge of 'black' absorption troughs in saturated resonance lines (e.g., Groenewegen et al. 1989), or the velocity (and widths) of asymptotic narrow absorption components (e.g., Prinja et al. 1990).

These diagnostics can also be applied to the UV spectra of luminous B supergiants. Using these methods we have obtained terminal velocities in the range $\sim$2000 to 250 km s$^{-1}$ for types B0–B5. A summary of the mean values per spectral bin is given in Table 1. The mean velocities decline steeply from B0 to B5, with some suggestion that the weaker winds of (the less luminous) Ib stars are faster for a given spectral type. The diagnostic value of the velocity difference, $v_{\rm edge} - v_\infty$, remains to be established, and is shown in Fig. 1 for stars in our survey. The maximum blue-edge velocity of B supergiants can exceed $v_\infty$ by up to $\sim$800 km s$^{-1}$, and it is perhaps not surprising that larger velocity differences are apparent in the well developed, extended profiles of the most luminous stars. The large scatter in values of $v_{\rm edge} - v_\infty$ in Fig. 1 is principally due to the fact that $v_{\rm edge}$ is highly time-variable.

The photospheric escape velocities ($v_{\rm esc}$) of the B0–B5 stars are plotted in Fig. 2a against the measured terminal velocities. Also shown are the 'PPK' predictions using the standard prescriptions of Pauldrach et al. (1986). As has been previously noted (e.g., Lamers et al. 1995), the observed terminal velocities of

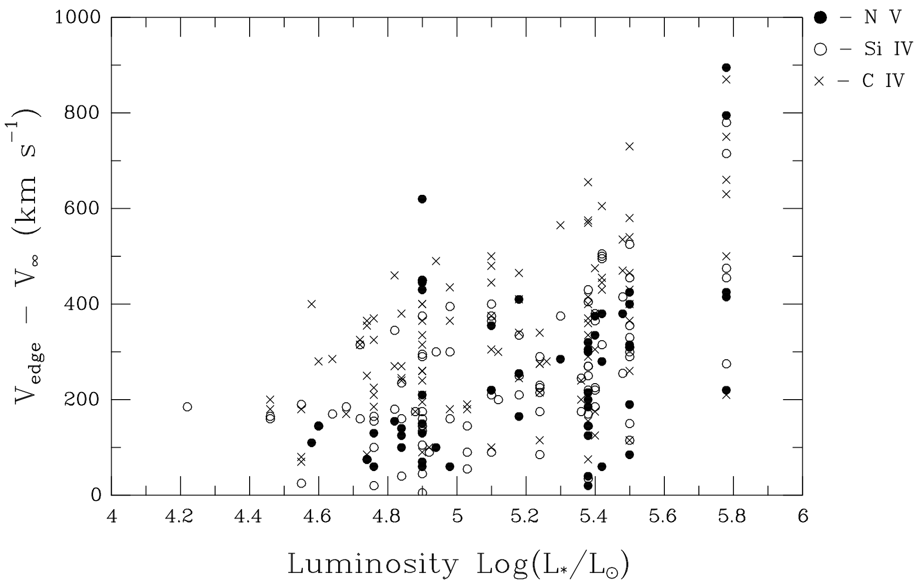


Figure 1. The velocity difference between the maximum observed blue edge ($v_{\rm edge}$) and the terminal velocity, $v_\infty$, plotted against stellar luminosity for N V, Si IV, and C IV resonance lines.

B supergiants are generally lower than those predicted by the 'standard' models, with the most glaring discrepancies (more than 50%) at spectral types B2 and later. (We adopt the effective-temperature scales of Humphreys & McElroy 1984, plus stellar masses interpreted from the grids of Schaller et al. 1992.)

The ratio of $v_\infty/v_{\rm esc}$ is plotted in Fig. 2b as a function of effective temperature; also added here are data for O-type stars (crosses), using only the '$v_{\rm black}$' values of Prinja et al. (1990). The $v_\infty/v_{\rm esc}$ values of O stars do not depend strongly on $T_{\rm eff}$, with a mean value of $\sim$2.53 (s.d. 0.36). For spectral types later than $\sim$B2 ($\log T_{\rm eff} \leq 4.3$), $v_\infty/v_{\rm esc}$ has a dependence on temperature of the form $v_\infty/v_{\rm esc} = 5.43\log(T_{\rm eff}) - 21.5$. The region between types B1–B2 ($\log T_{\rm eff} \sim$ 4.3–4.35) is sometimes referred to as the 'bi-stability jump' (e.g., Lamers et al. 1995), where a drastic change in the nature of the wind-driving lines is predicted (Pauldrach & Puls 1990), depending on whether the winds are optically thick or thin in the Lyman continuum. Our measures (Fig. 2b) suggest that this region is marked by a considerably greater observed spread in $v_\infty/v_{\rm esc}$ values (mean value $\sim$2.30; s.d. 0.55); this spread somewhat smears out the starkness of the discontinuity or 'jump'. The stars with $\log(T_{\rm eff}) \sim$4.31 (i.e., B1 Ib) provide a fine illustration of the scatter in $v_\infty/v_{\rm esc}$ at a given temperature (Fig. 2b). The ratio of C II $\lambda$1335 to C IV $\lambda$1550 wind emission strengths for all B1 Ib stars in our sample is plotted in Fig. 3 as a function of the terminal velocity. (We used UV spectra of B1 giants to provide a template or reference for these measures.) The data in Fig. 3 confirm the strong correlation between the degree of ionization in the wind and $v_\infty$ near the bi-stability region (see Lamers et al. 1995). There is a shift from high to low ions corresponding to a

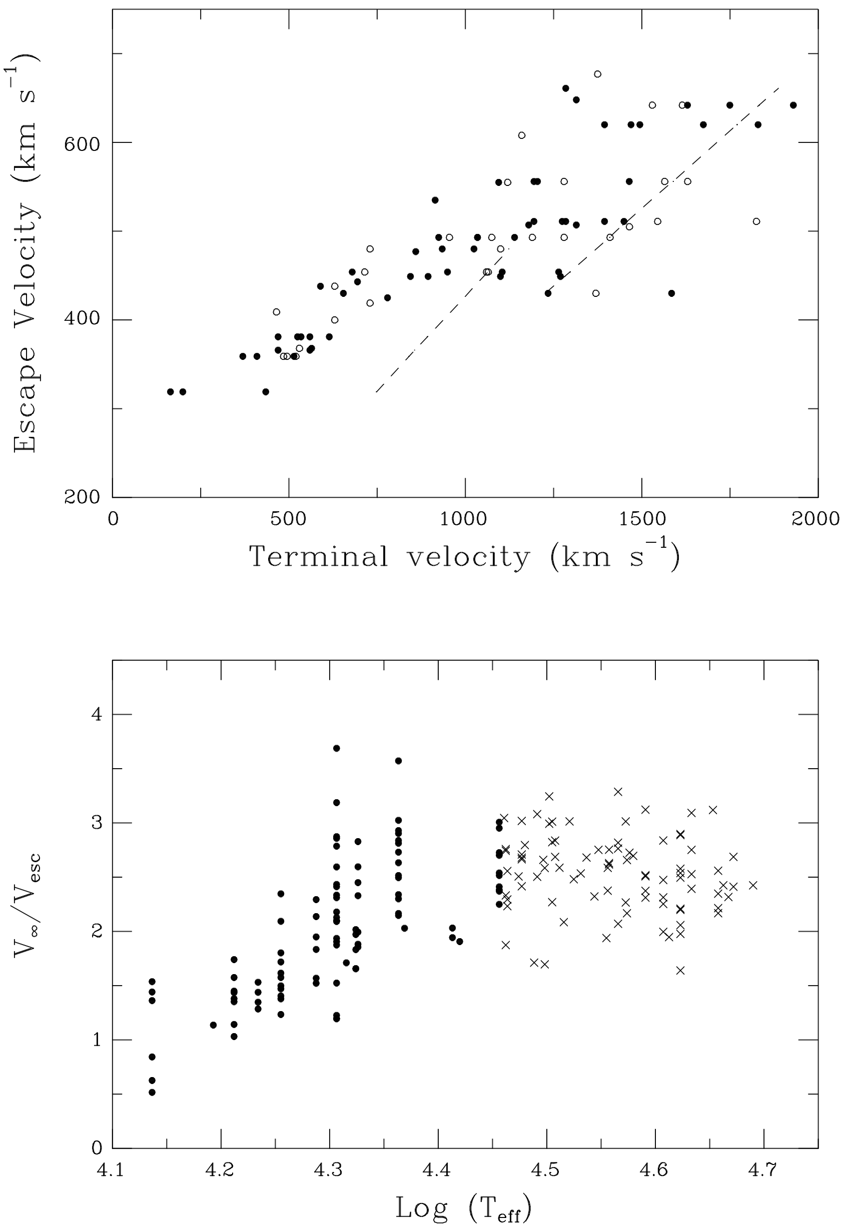


Figure 2. (a) Upper panel: The photospheric escape velocity ($v_{\rm esc}$) plotted against $v_\infty$ for B0–B5 supergiants. The terminal velocities are measured from the violet limits of saturated troughs (filled circles) or the asymptotic central velocities and half-widths of narrow absorption components (open circles). The dashed lines are the predicted values for the 'standard' PPK relations. (b) Lower panel: the ratio of $v_\infty/v_{\rm esc}$ against $\log T_{\rm eff}$. Data from saturated O-star profiles are added (crosses) from Prinja et al. (1990).

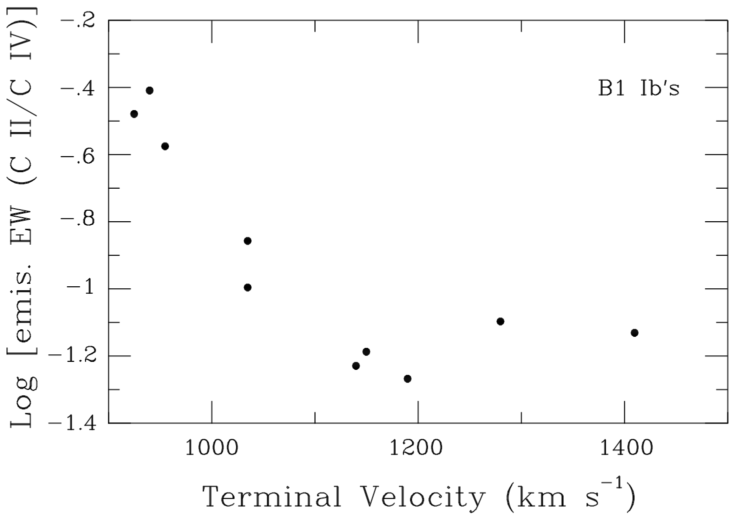


Figure 3. The observed ratio of emission strengths for C II $\lambda$1335 and C IV $\lambda\lambda$1550 plotted against the $v_\infty$ for stars of spectral type B1 Ib only (i.e., $T_{\rm eff} \simeq 20\,400$ K. See also Lamers et al. 1995).

shift from high to low observed wind velocities. Ultimately it will be interesting to compare the mass-loss rates of stars in this region.

It is reasonable to suggest that some of the scatter in $v_\infty/v_{\rm esc}$ in Fig. 2b – at spectral types *other* than B1 – is due to an additional physical mechanism, perhaps stellar rotation (e.g., Friend & Abbott 1986; Friend 1990). The ratio of $v_\infty/v_{\rm esc}$ for B0 to B5 stars is plotted in Fig. 4 against the ratio of projected rotation velocity ($v_{\rm e} \sin i$) and critical velocity ($v_{\rm crit}$, which is the equatorial velocity at which the centrifugal force matches the gravitational force). These data do not, however, provide any compelling evidence that $v_\infty/v_{\rm esc}$ is strongly affected by stellar rotation, especially when the 'outlying' stars $\gamma$ Ara (highly exceptional two-component wind; Prinja et al. 1997) and the massive early-type binaries V861 Sco (Bunk & Haefner 1991) and HD 93827 (Garrison et al. 1983) are excluded.

## 3. Mass-Loss Rates and Ion Fractions

In order to determine the absorption optical depths, wind densities, and relative ionization behaviour of B supergiants, we have used the SEI model profiles for spherically symmetric winds (Lamers et al. 1987) to match the observed wind lines. In addition, however, we adopt the modifications to this code described by Massa et al. (1995), where the radial optical depth, $\tau_{\rm rad}(w)$, is treated in ten independent variable bins. This arbitrary approach is preferred simply to sample observed absorption optical depths in winds which are in fact highly structured and time-variable. For the B0–B1.5 stars in our sample we adopted input photospheric spectra based on rotationally broadened IUE spectra of cor-

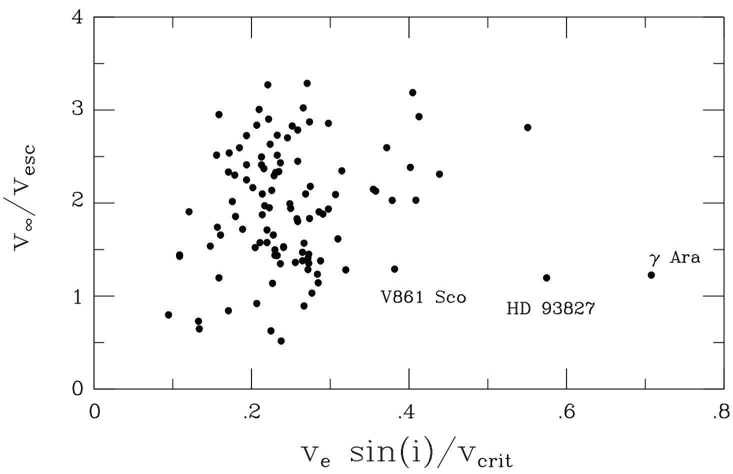


Figure 4. The ratio of $v_\infty/v_{\rm esc}$ versus the ratio of projected to critical rotational velocity for spectral types B0–B5. Three exceptional 'outlying' stars are labelled (see text).

responding low $v_{\rm e} \sin i$ main-sequence stars. Giant-star spectra were used for types B2–B5. We discuss here principally the results from our profile fits to the Si IV $\lambda\lambda$1400 and C IV $\lambda\lambda$1550 resonance-line doublets, which can be traced down to B5. Generally, good matches are obtained to the observed profiles down to velocities $\sim 0.3v_\infty$. At much lower velocities the SEI models predict insufficient absorption (or an excess emission), which may relate for instance to the presence of non-monotonic outflows, assumption of the 'core-halo' model, and inadequacies in the input photospheric spectra (see, e.g., Massa et al. 1995).

The products of mass-loss rate and ion fraction ($\dot{M}\, q_i$), calculated at $w = 0.5v/v_\infty$ from the SEI model fits, are shown in Fig. 5 for C IV and Si IV. In both cases the unsaturated profiles (detections) indicate (the expected) strong dependence on luminosity, which for C IV is of the form $\dot{M}\, q({\rm C}^{3+}) = 1.4 \log(L/L_\odot) - 16.7$ for B0–B5 stars (cf. O-star results of Howarth & Prinja 1989).

Only one B supergiant in our sample ($\epsilon$ Ori) has a reliable radio mass-loss rate, so the product $\dot{M}\, q_i$ cannot be reliably split. Using the empirical mass-loss versus luminosity prescription for Galactic supergiants given by Lamers & Cassinelli (1996) yields values for the mean ion fractions, $\overline{q}({\rm C}^{3+}) = 0.5 \times 10^{-3}$ and $\overline{q}({\rm Si}^{3+}) = 1.0 \times 10^{-3}$. The individual ion fractions (based on these empirical mass-loss rates) are plotted in Fig. 6 as a function of effective temperature. There is a slight indication that both ion fractions peak close to spectral types B1, before decreasing towards the O-star temperatures. The relative ion ratio, $q({\rm C}^{3+})/q({\rm Si}^{3+})$ is plotted in Fig. 7, for values calculated at $w = v/v_\infty = 0.5$, 0.7, and 0.8–0.9. (We show here the dependence on luminosity which is surprisingly stronger than that evident against effective temperature.) The ratios are essentially similar for a given stellar luminosity, and it is clear then that the relative ion mixture in the stellar winds of B0–B5 stars is very stable between 0.5 and $0.9v_\infty$, or $\sim$2–10 stellar radii.

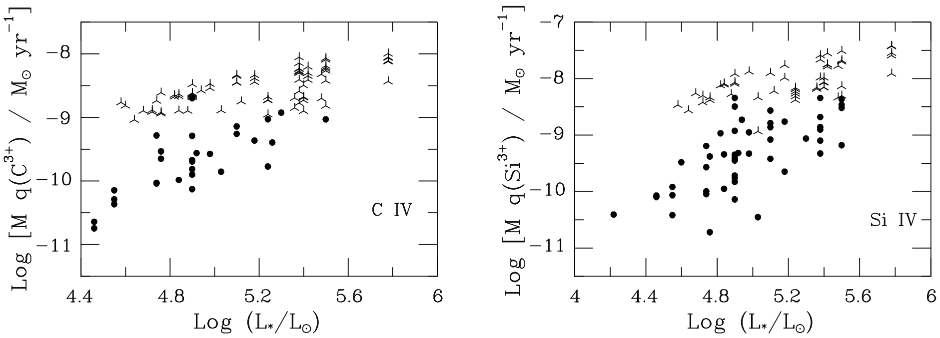


Figure 5. The products of mass-loss rate and ion fraction derived from SEI-model profile fits are plotted against stellar luminosity for C IV and Si IV. The filled circles are 'detections' (unsaturated profiles); lower limits are indicated for numbers derived from saturated profiles. A similar dependence on luminosity is apparent for both lines.

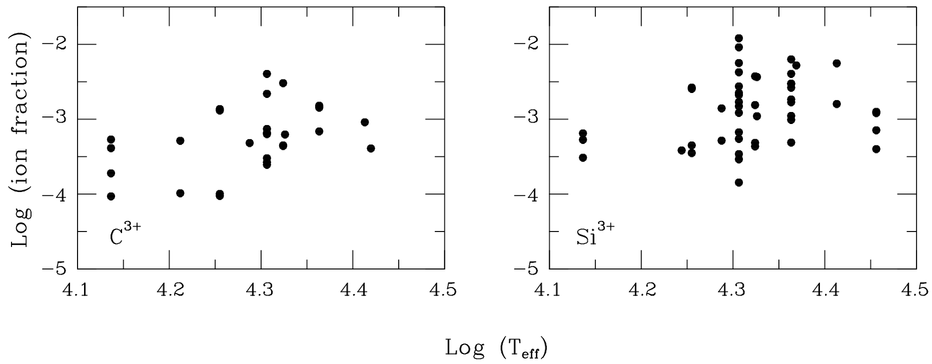


Figure 6. The ion fractions $q(C^{3+})$ and $q(Si^{3+})$ versus log of the effective temperature for spectral types B0–B5. Empirical mass-loss rates from Lamers & Cassinelli (1996) have been adopted.

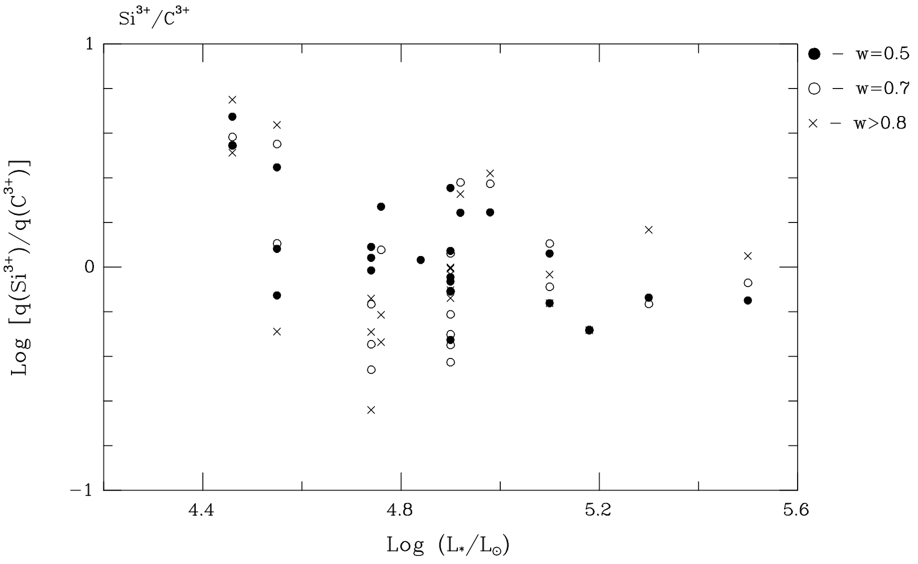


Figure 7. The ion ratio $q(\mathrm{Si}^{3+})/q(\mathrm{C}^{3+})$ determined at three wind velocities is plotted against luminosity.

We are currently pursuing SEI-profile modelling of low-ion species, including Si II $\lambda$1527 and Si III $\lambda$1207, which will then combine with results for Si IV $\lambda\lambda$1400 to highlight the dominance (at early-B types) of Si V.

## 4. Dynamic Photospheres

Previously, Massa et al. (1992) have demonstrated that the Si III $\lambda\lambda$1300 'photospheric' multiplet in B1 stars becomes more asymmetric with increasing luminosity (and mass-loss). Systematic velocity shifts are also present in the strong Si III singlets at $\lambda$1312 and $\lambda$1417, thus providing evidence for photospheric velocity gradients. In our survey we find evidence to support these effects down to spectral types B5. The observed velocity shifts between Si III $\lambda$1299 and C II $\lambda$1324 (which is expected to form much deeper in the atmosphere) are shown in Fig. 8, separating between Ia and Ib classes in spectral bins down to B5. Each spectral bin reveals greater (blueward) velocity shifts (of up to 30 km s$^{-1}$) for the more luminous B stars. These results imply that the photospheres of B0–B5 stars are affected by radial expansion (they are dynamic), with ultimate consequences for the construction of B-star photospheric models, the inclusion of microturbulence, and for accounts of the near-star stellar winds.

## 5. Summary of Main Results

1. The terminal velocities decline sharply from ~2000 to 200 km s$^{-1}$ between types B0 to B5. The maximum observed (blue) edge velocities of satu-

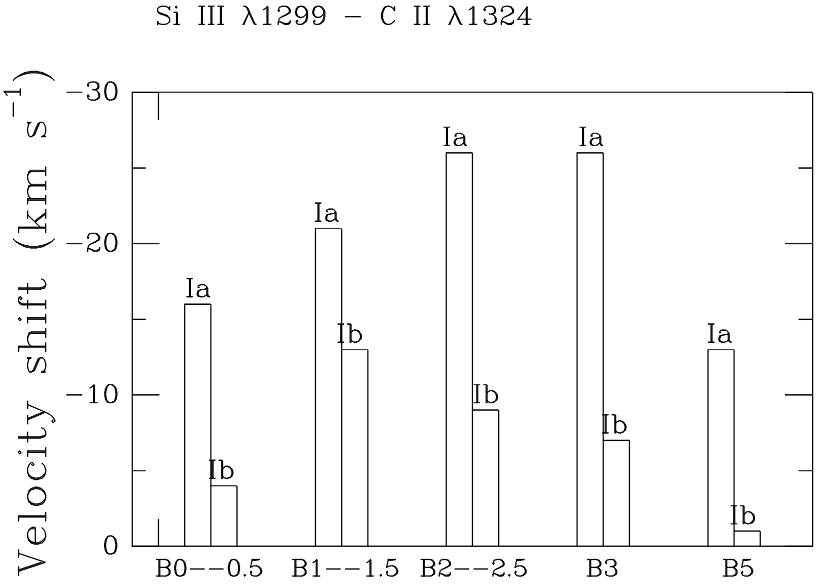


Figure 8. The measured velocity shifts between the Si III $\lambda$1299 and C II $\lambda$1324 photospheric lines; the photospheres of B supergiants are dynamic

rated resonance lines can exceed $v_\infty$ by up to ~800 km s$^{-1}$, with a weak dependence on luminosity.

2. The observed $v_\infty$ values for B2 and later type stars are discrepant from the standard 'PPK' prescriptions by more than 50%.

3. The region of the 'bi-stability jump' is marked by a considerably greater spread in the observed ratio of $v_\infty/v_{\rm esc}$; e.g., at B1 types this ratio may vary between ~1.2 and 3.7.

4. SEI-model profile fits confirm a strong luminosity dependence for the product of mass-loss rate and ion fraction for C IV and Si IV. Adopting empirical mass-loss rates gives mean ion fractions, $\overline{q}(\mathrm{C}^{3+}) = 0.5 \times 10^{-3}$ and $\overline{q}(\mathrm{Si}^{3+}) = 1.0 \times 10^{-3}$.

5. The relative ion mixture of the winds of B0–B5 stars does not change substantially as a function of velocity, between $\sim 0.5$ and $0.9 v_\infty$.

6. Velocity shifts of up to ~30 km s$^{-1}$ are apparent in the photospheric lines, thus pointing to the incidence of photospheric velocity gradients down to B5.

**Acknowledgments.** We are grateful to NATO for financial support for this project.

### References

Bunk, W., Haefner, R., 1991, A&A, 251, 515

Friend, D. B., 1990, ApJ, 353, 617

Friend, D. B., Abbott, D. C., 1986, ApJ, 311, 701

Garrison, R. F., Schild, R. E., Hiltner, W. A., 1983, ApJS, 52, 1

Groenewegen, M. A. T., Lamers, H. J. G. L. M., 1989, A&AS, 79, 359

Groenewegen, M. A. T., Lamers, H. J. G. L. M. Pauldrach, A. W. A., 1989, A&A, 221, 78

Howarth, I. D., Prinja, R. K., 1989, ApJS, 69, 527

Humphreys, R. M., McElroy, D. B., 1984, ApJ, 284, 565

Lamers, H. J. G. L. M., Cerruti-Sola, M., Perinotto, M., 1987, ApJ, 314, 726

Lamers, H. J. G. L. M., Snow, T. P., Lindholm, D. M., 1995, ApJ, 455, 269

Lamers, H. J. G. L. M., Cassinelli, J. P., 1996, in From Stars to Galaxies: The Impact of Stellar Physics on Galactic Evolution (ASP Conf. Series), eds. C. Leitherer, U. Fritze-von Alvensleben & J. Huchra (ASP, San Francisco), p. 162

Lucy, L. B., 1982, ApJ, 255, 278

Lucy, L. B., 1983, ApJ, 274, 372

Massa D., Shore, S. N., Wynne, D., 1992, A&A, 264, 169

Massa D., Prinja, R. K., Fullerton, A. W., 1995, ApJ, 452, 842

Owocki, S. P., Castor, J. I., Rybicki, G. B., 1988, ApJ, 335, 914

Pauldrach, A., Puls, J., Kudritzki, R. P., 1986, A&A, 164, 86

Pauldrach, A., Puls, J., 1990, A&A, 237, 409

Prinja, R. K., Barlow, M. J., Howarth, I. D., 1990, ApJ, 361, 607

Prinja, R. K., Massa, D., Fullerton, A. W., Howarth, I. D., Pontefract, M., 1997, A&A, 318, 157

Schaller, G., Schaerer, D., Meynet, G., Maeder, A., 1992, A&AS, 96, 269

### Discussion

**Kudritzki:** My original ambition was to come here with a new calibration of $v_\infty/v_{\rm esc}$, but of course I ran out of time...
**Prinja:** Well, I look forward to seeing it soon!